

A SIMPLE NON-LINEAR MODEL FOR THE EFFECT OF PARTIAL SHADE ON PV SYSTEMS

Niket Thakkar, Daniel Cormode, Vincent P.A. Lonij, Steve Pulver and Alexander D. Cronin
University of Arizona, Tucson, AZ, USA

ABSTRACT

The effect of shade from one PV module on another is incorporated into a model for the power generated by PV systems. The model is calibrated with data from the Tucson Electric Power solar test yard. Shade de-rating factors from the model are compared with data every minute of the day and every day of the year. The model is then used to predict final yields (kWh/kW_{DC}) for different PV system deployments with various (non-tracking) module orientations and ground-cover ratios. Several heuristics are put forth to help understand how the observed non-linear response to shade can impact the yield from PV systems. In one example, we find that a PV system deployed in the Tucson Electric Power solar test yard could produce 22% more kWh for the month of December (and 3.8% more annually) if the modules were separated by twice as much distance. In another example, we predict that a system in Tucson with south-facing modules at 12-degrees from horizontal can generate 1.5 times as many kWh/yr per square-meter of land compared to a system with modules at 32-degrees (the latitude angle). These examples emphasize the non-linear impact of partial shade on PV system performance.

INTRODUCTION

The impact of shadows on PV systems is often underestimated because PV systems respond nonlinearly to shade. Several references discuss nonlinear responses for individual modules. However, this response to shade is largely ignored in literature describing the performance of PV systems with multiple rows of panels. Because an analysis of how PV systems respond to shade is important for optimizing final yields, predicting de-ratings, and designing new PV system deployments, we have developed and tested a model for the non-linear effect of partial shade on PV systems.

In this paper we describe how PV systems at the Tucson Electric Power (TEP) solar test yard respond to shade from neighboring rows of solar panels. We show data and a model for the PV output every minute of the year (see figure 1), and we report results from shading experiments that were done to verify the model presented here. We identify one particular PV system found at the TEP test yard that could yield 22% more energy in December (and 3.8% more energy annually) if it were re-positioned to reduce the amount of shade that falls on its modules from neighboring rows of PV strings. Unlike many mathematical models of partial shade on PV arrays, our model has a relatively simple analytical expression and is therefore

easily used to model different arrays. We conclude by offering a few extrapolations and heuristics regarding the impact of partial shade on PV arrays.

First we review some literature on this topic. The fraction of a solar array that is covered by shadows, often defined as the 'shade factor', is discussed in numerous articles [1-8]. Many of these articles invoke different models for diffuse irradiance, some consider tracking modules, and some consider shade from fences, trees, poles, or neighboring modules. However none of the models in references [1-8] incorporate the nonlinear response of solar modules to partial shade.

On the other hand, the nonlinear effect of shade on individual PV modules has been studied in several references [9-13] that describe how shading one cell out of twenty can reduce the output of a module by a fraction much larger than 1/20. References [9-13] focus on bypass diodes, equivalent circuit models, or methods for maximum power point tracking. But references [9-13] do not explicitly predict how entire PV systems with arrays of panels will perform throughout the day.

A few PV system performance reviews [14-20] describe the effect of shade on entire systems. Some discuss 'shade impact factor' as a way to quantify the disproportionately large reduction in power that results from partial shading. But none of these reviews give a closed-form analytical expression such as the one presented here.

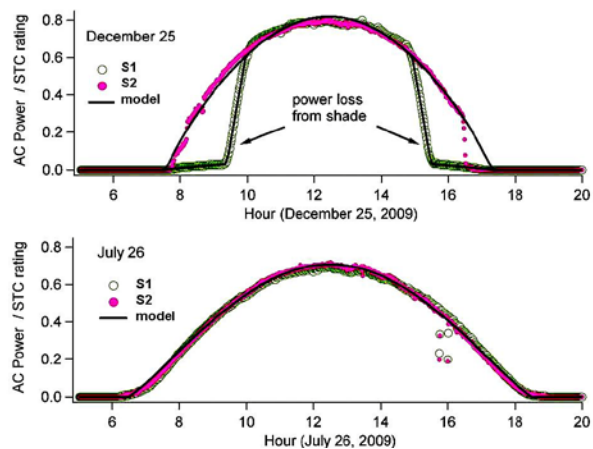


Figure 1: (Top) AC Power output from two PV systems on 12/25/2009. System S1 (open circles) has modules that get shaded in mornings and evenings. (Bottom) the same two systems' output on 7/26/2009.

SHADE DE-RATING

Figure 1 shows the AC power output from two PV systems every minute of the day on 12/25/2009 and 7/26/2009, two nearly cloudless days in Tucson. Also shown in Figure 1 is the result of our model, with different shade de-ratings for the two PV systems. The output from system S1 is severely affected by shading for two hours in the morning, and again in the evening. S1 effectively turns on late and turns off early. The missing hours of power from S1 are due to shade on just a small part of the modules. A photograph of shadows covering part of system S1 is shown in Figure 2.

System S1 has 16 poly-crystalline silicon modules made by Sharp, each with an STC peak-power rating of 165 W (2640 W total), and an Aurora inverter. System S2 is composed of 9 mono-crystalline silicon 215 W SunPower modules (1935 W total) and a Sunyboy inverter. Both systems are mounted at the TEP solar test yard in Tucson, Arizona at the latitude angle (32°) facing south. Both systems' modules have only 3 bypass diodes, allowing columns (not rows) of cells to be bypassed.

To compare the power output from the two systems in figure 1, the AC power was measured every 1-minute with a revenue-grade power meter made by ABB. The final yields (measured AC power / STC rating) for each system are then plotted.



Figure 2: PV systems with shade from one row on another. (Top) Modules from system S1 at the TEP solar test yard photographed 12/14/2009 at 3:05 pm (photo by Alex Cronin). (Bottom) The shaded length (a) is found from the intersection of lines 1 and 2.

The two systems get different amounts of shade. System S1 is north of some rows that periodically shade its modules as shown in Figure 2. System S2 has modules in a front row that rarely get shaded, although the abrupt loss of power on 12/25/2009 at 4:30 pm from S2 is due to shade from a building 40 meters away.

Our theoretical model is compared to the data in Figure 1. The model is based on a solar position algorithm, an attenuating (but cloudless) atmosphere, the geometry shown in Figure 2, and the observation that the most weakly illuminated row of cells limits the power from an entire string of PV modules. We verified this response to shade empirically by covering portions of every module at the TEP solar test yard for a few minutes.

Completely shading one row of cells (typically only 1/14 of a module's length) reduces the output of most PV systems by 100%. We use the observation that the AC electrical output power is proportional to the radiant power incident on the most weakly illuminated row of cells. This response to shade is plotted in Figure 3, and we emphasize that it is non-linear in the shaded area of the module. There are exceptions to this rule, based on bypass diodes, shunt resistance values, and landscape vs. portrait orientation of the modules. But this remarkably simple rule - output dominated by the most weakly illuminated row of cells - describes our observations quite well. This claim is supported by the data shown in Figures 1, 2, 3, and 5.

The power produced by each PV system is predicted by

$$P = \Gamma \times (\hat{S} \cdot \vec{A}) I_0 \eta \exp \left[-\frac{\alpha}{\hat{u}p \cdot \hat{S}} \right] \quad (1)$$

where Γ is the reduction factor due to partial shading, \hat{S} is the unit vector pointing to the sun, \vec{A} is the area vector normal to the modules, I_0 is the solar constant, η is the system efficiency, α is the atmospheric attenuation for one air mass, and $\hat{u}p$ is a unit-vector pointing to the zenith. The shade de-rating factor Γ is found from the shaded portion of each module (a) as compared to cell size (c) according to

$$\Gamma = \min \left(1, \max \left(0, 1 - \frac{a}{c} \right) \right) \times .94 + 0.06 \quad (2)$$

The factor 0.06 approximates the diffuse irradiance (mostly sky light) still incident on the panel when shade from neighboring rows begins to reduce output. The amount of each module that is shaded (a) is found from the intersection of the two lines labeled in Figure 2. The shaded length a is given by

$$a = \frac{L \sin(\theta) - m_1 s}{m_1 \cos(\theta) + \sin(\theta)} \quad (3)$$

$$m_1 = -\frac{\hat{S} \cdot \hat{u}p}{\hat{S} \cdot \text{south}} \quad (4)$$

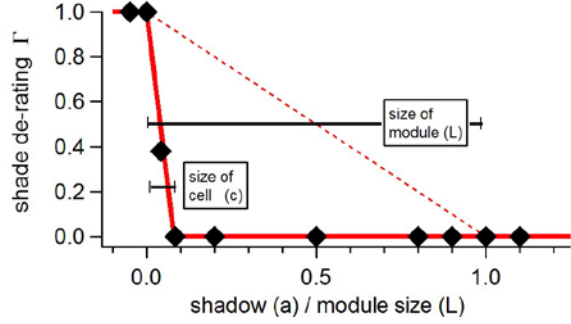


Figure 3: Graph of the shade de-rating factor Γ . Diamonds are empirical data points from deliberately shading portions of PV modules. The model Γ (solid red line) describes typical PV systems with $c = L/14$. The dashed model is for an optimistic case given $c = L$.

The length of the module (L), the angle of the modules (θ), and the map-view separation between modules (s) are all fixed parameters. But because \hat{s} changes with time, therefore m_1 , a , and Γ also depend on time.

The system efficiency η also changes with time, mostly due to temperature. In our model we used η from STC ratings with an additional de-rating that is found empirically from the TEP data to vary from 0.77 in winter to 0.61 in summer. For simplicity, we used a sinusoidal de-rating

$$\eta = \eta_{STC} (0.61 + 0.08 [\cos(2\pi t/\text{year}) + 1]) \quad (5)$$

where t is time in years since Jan 20. This one-month lag from the winter solstice allows, empirically, for temperature de-ratings throughout the year. For S1, $\eta_{STC} = 14\%$, and for S2, $\eta_{STC} = 17\%$.

For completeness, we explain the simple (circular orbit) solar position algorithm that we use [21]. In the rotating equatorial reference frame $\hat{s} = (S_x, S_y, S_z)$ is given by:

$$S_x = \cos(23^\circ * \sin(2\pi t/\text{year})) \sin(2\pi t/\text{day}) \quad (6)$$

$$S_y = \cos(23^\circ * \sin(2\pi t/\text{year})) \cos(2\pi t/\text{day}) \quad (7)$$

$$S_z = \sin(23^\circ * \sin(2\pi t/\text{year})) \quad (8)$$

and $\hat{u}_p = (U_x, U_y, U_z)$ is given by:

$$U_x = \cos(\text{latitude}) \quad (9)$$

$$U_y = 0 \quad (10)$$

$$U_z = \sin(\text{latitude}) \quad (11)$$

This model is then used to calculate daily final yields (kWh/kW) for systems with and without partial-shading, as shown in Figure 4. The ratio between these final yields highlights how the de-rating due to shade changes throughout the year. This is shown, and compared to data for the ratio of final yields in Figure 5.

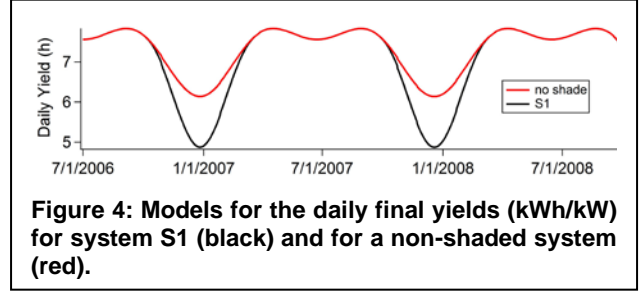


Figure 4: Models for the daily final yields (kWh/kW) for system S1 (black) and for a non-shaded system (red).

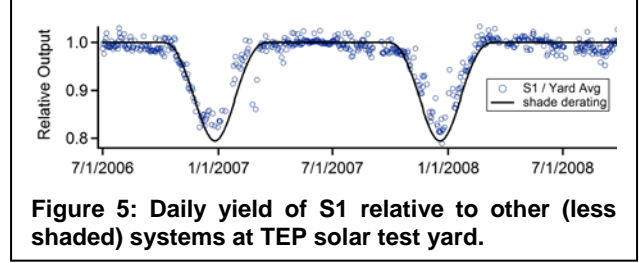


Figure 5: Daily yield of S1 relative to other (less shaded) systems at TEP solar test yard.

Because the model ignores clouds, it is only expected to be valid for sunny days. That is why we chose to compare relative daily final yields in Figure 5. The ratio of final yields is a simple way to remove the large fluctuations in daily final yields due to cloudy days.

To summarize this section, we have described a simple mathematical model for PV system de-rating due to partial shade from neighboring rows. Figure 1 indicates how well this model works each minute of the day, and figure 5 indicates how well the model works for each day of the year. Now we can use this model for several more predictions

DISCUSSION

Using this model we have predicted the annual final yield for latitude-tilt systems in Tucson as a function of the spacing s between rows (Figure 6). Rather than assume a particular panel length, we plot the annual final yield vs. the ratio s/h , where h is the height of the module ($h = L \sin \theta$). We show two curves in Figure 6: one with the severe sensitivity to shading that is typical of most PV systems (described by $c = L/14$) and one more optimistic plot (using $c = L$).

From similar analysis, we find that S1 could produce 22% more kWh for the month of December and 3.8% more annually, if the panel separation s were increased by one meter. For many purposes 3.8% is not a large loss. However, the particular system S1 that we used to experimentally test our model is an example of a PV system that was constructed by a professional PV system installation crew and had no constraints requiring such spacing. To prevent even larger de-ratings due to shade, we recommend using a model such as ours.

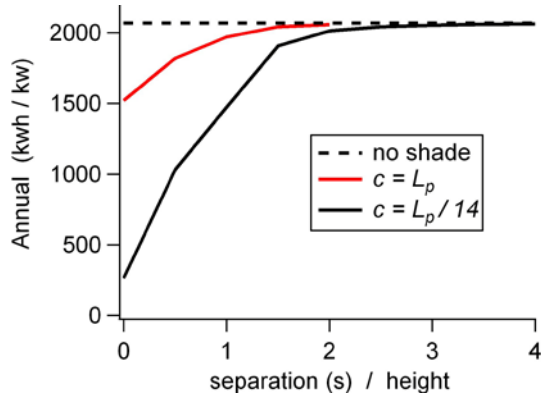


Figure 6: De-rating due to shade for latitude-tilt modules in Tucson as a function of the row separation. A typical system with cell size $c = L/14$ (black) has a larger de-rating than the optimistic model with cells size $c = L$ (red).

Figure 7 shows the space we recommended between modules to keep the shade de-rating factor smaller than a 5% loss for the annual kWh. The space between rows depends on the row height and the latitude of the system. For Figure 7 we have assumed fixed-angle latitude-tilt rows of modules for different latitudes. Again, significantly different results are found for the realistic case with cell size $c = L/14$ as compared to the optimistic case of $c = L$.

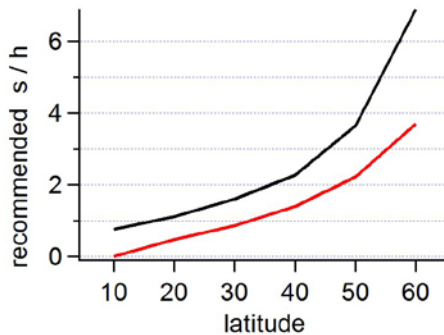


Figure 7: Recommended space between rows to maintain 95% of the annual shade-free kWh. Typical PV systems with cell size $c = L/14$ (black) require more space between rows than the optimistic case with $c = L$ (red).

As a further extrapolation, we use the same model to predict yields per land-area. To compare deployments with different angles, we consider toe-to-toe spacing of the rows, as opposed to the separation between rows. This metric is known as 'ground cover ratio', i.e. the ratio of land area to module area [20]. Figure 8 shows annual outputs in Tucson for PV systems with modules at 32° , 12° , and 0° and $\eta_{STC} = 10\%$. The highest annual kWh per land area is obtained from horizontal panels laid closely together. This is because tilted horizontal (0°) panels never shade each other and they receive all the sunlight incident on the land. (We caution again at this point that

differences in soiling and temperature effects due to module orientation are ignored in our model so far).

Taking into account the space between modules that is needed to keep 95% of the shade-free annual yield, we find that 1 MW of Sharp modules oriented at 32° could be deployed in 3.0 Acres and would yield slightly more than 2000 MWh per year (with no clouds). This uses a ground cover ratio of 1.7. Figure 7 shows how 1.4 times as much energy yield (2800 MWh) could be generated on the same 3.0 Acres of land if the modules were tilted at 12° . This uses a ground cover ratio of 1.2.

Figure 9 tells a different aspect of the story. Here, we plot PV system annual yields per module area. In this case, we see that panels tilted at 32° can generate slightly more MWh per year than those at 12° .

To optimize the module tilt angle θ requires additional constraints such as the cost of land and conduit as compared to the cost of modules and mounting hardware. Our main point here is that a realistic model of non-linear de-rating due to shade should be taken into account when selecting module spacing.

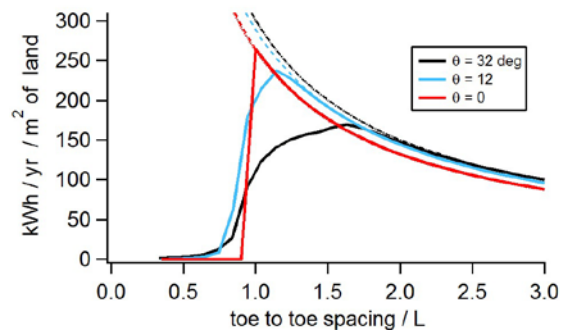


Figure 8: Annual kWh output per land area, plotted as a function of the space between rows for modules with different (fixed) tilt angles θ .

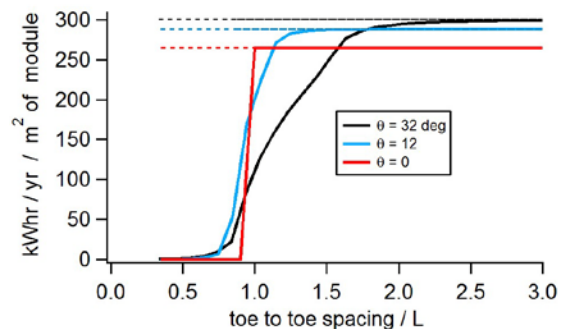


Figure 9: Annual kWh output per module area. Shade de-ratings are significant when rows of modules are too close together.

INTERPRETATION

Since the most weakly illuminated row of cells limits the performance of entire PV systems, it is important to consider the view of the sky as seen from the bottom of a module. In Figure 10 we present an altitude-azimuth (alt, az) view of the back side of other modules using the equation

$$alt = \text{atan}\left(\frac{h \cos(az)}{s}\right) \quad (12)$$

The solid black line in Figure 10 indicates the view from the bottom of the modules of System S1. The dashed black line indicates the view from a location one cell up from the bottom.

Also plotted in Figure 10 are the sun-paths each month, with markers every hour. This plot shows how many hours each month the neighboring rows of modules cast shadows on the bottom cells of a module.

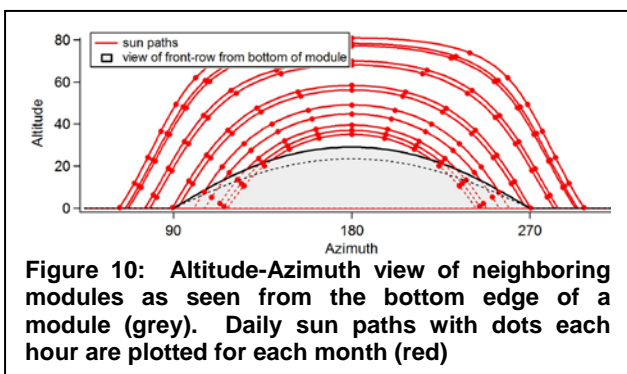


Figure 10: Altitude-Azimuth view of neighboring modules as seen from the bottom edge of a module (grey). Daily sun paths with dots each hour are plotted for each month (red)

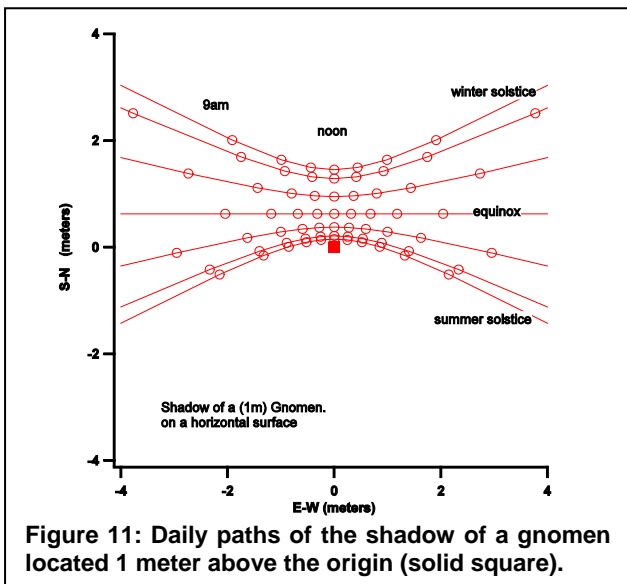


Figure 11: Daily paths of the shadow of a gnomon located 1 meter above the origin (solid square).

A related plot is shown in Figure 11, where the daily paths of the shadow of the top of a 1-meter tall stick (a gnomon) are plotted, with markers every hour, for the first seven months of the year. This plot indicates how far to the north the next row of modules should be placed in order to avoid shadows.

As one final point we note that increases in power output due to concentrating sunlight on typical PV modules, for example by positioning diffuse reflectors around the modules, are limited by a similar de-rating factor. Because the least illuminated cells tend to limit the current and hence the electrical power output, a similar de-rating factor as the one discussed here can be used to more realistically quantify the benefit of concentration schemes.

Table 1: Recommended separation between rows of latitude-tilt modules keep to shade de-rating below 5% loss, given our model with $c=L/14$ (typical modules) and for comparison $c=L$ (optimistic case).

Latitude	s/h given $c=L/14$	s/h given $c=L$
10	0.8	0.0
20	1.1	0.5
30	1.6	0.9
40	2.3	1.4
50	3.7	2.2
60	6.9	3.7

SUMMARY

Partial shade reduces yields from PV systems more than several models would predict. This is due to a non-linear response to shade that is observable for most PV systems. For example, the power from a 2.6 kW grid-tied PV system in Tucson is shown to drop by 94% when shadows from one row of modules fall on only 8% of the surface area of the next row of modules. This large de-rating due to a small amount of shade is described in a simple model presented in this paper.

Our mathematical de-rating factor due to partial shading of PV systems by neighboring rows of modules was presented. Our model was calibrated with data from the Tucson Electric Power solar test yard. We demonstrated how this model can be used to predict the recommended spacing between rows of modules at different latitudes, different orientations, and different cell sizes. The fact that PV systems can be severely hindered by a small amount of shade makes this type of model particularly important when designing PV systems or analyzing PV system data.

ACKNOWLEDGEMENTS

We acknowledge Tucson Electric Power for providing access to the solar power test yard. We acknowledge the Arizona Research Institute for Solar Energy (AZRISE) for financial support. We acknowledge N. Davidson and R. Price for help acquiring the data presented here.

REFERENCES

- [1] J. Appelbaum and J. Bany, Shadow effect of adjacent solar collectors in large scale systems, *Solar Energy* 23, 497 (1979).
- [2] J. Bany and J. Appelbaum, The effect of shading on the design of a field of solar collectors, *Solar Cells* 20, 201 (1987).
- [3] M. Drif, P. Perez, J. Aguilera, and J. Aguilar, A new estimation method of irradiance on a partially shaded PV generator in grid-connected photovoltaic systems, *Renewable Energy* 33, 2048 (2008).
- [4] M. Elsayed, Monthly-averaged daily shading factor for a collector field, *Solar Energy* 47 (1991).
- [5] M. Elsayed and A. Al-Turki, Calculation of shading factor for a collector field, *Solar Energy* 47, 413 (1991).
- [6] P. Groumpos and K. Khouzam, A generic approach to the shadow effect of large solar power systems, *Solar Cells* 22, 29 (1987).
- [7] R. Jones Jr. and J. Burkhart, Shading effects of collector rows tilted toward the equator, *Solar Energy* 26, 563 (1981).
- [8] D. Passias and B. Kallback, Shading effects in rows of solar cell panels, *Solar Cells* 11, 281 (1984).
- [9] M. Alonso-Garcia, J. Ruiz, and W. Herrmann, Computer simulation of shading effects in photovoltaic arrays, *Renewable Energy* 31, 1986 (2006).
- [10] J. Bishop, Computer simulation of the effects of electrical mismatches in photovoltaic cell interconnection circuits, *Solar Cells* 25, 73 (1988).
- [11] E. Karatepe, M. Boztepe, and M. Colak, Development of a suitable model for characterizing photovoltaic arrays with shaded solar cells, *Solar Energy* 81, 977 (2007).
- [12] V. Quaschnig and R. Hanitsch, Numerical simulation of current-voltage characteristics of photovoltaic systems with shaded solar cells, *Solar Energy* 56, 513 (1996).
- [13] E. Suryanto Hasyim, S. Wenham, and M. Green, Shadow tolerance of modules incorporating integral bypass diode solar cells, *Solar Cells* 19, 109 (1986).
- [14] R. Decker and U. Jahn, Performance of 170 grid connected PV plants in Northern Germany: Analysis of yields and optimization potentials, *Solar Energy* 59, 127 (1997).
- [15] E. Kymakis, S. Kalykakis, and T. Papazoglou, Performance analysis of a grid connected photovoltaic park on the island of Crete, *Energy Conversion and Management* 50, 433 (2009).
- [16] M. Sidrach-de Cardona and L. Lopez, Evaluation of a grid-connected photovoltaic system in southern Spain, *Renewable Energy* 15, 527 (1998).
- [17] J. So, Y. Jung, G. Yu, J. Choi, and J. Choi, Performance results and analysis of 3kW grid-connected PV systems, *Renewable Energy* 32, 1858 (2007).
- [18] S. Ubertini and U. Desideri, Performance estimation and experimental measurements of a photovoltaic roof, *Renewable Energy* 28, 1833 (2003).
- [19] A. Woyte, J. Nijs, and R. Belmans, Partial shadowing of photovoltaic arrays with different system configurations: literature review and field test results, *Solar Energy* 74, 217 (2003).
- [20] L. Navarrete and E. Lorenzo, Tracking and Ground Cover Ratio, *Prog. Photovolt: Res. Appl.* 16, 703 (2008).
- [21] A. Sproul, Derivation of the solar geometric relationships using vector analysis, *Renewable Energy* 32, pg. 1187-1205 (2007).